Reactions of Laser-Ablated Iridium Atoms with O_2. Infrared Spectra and DFT Calculations for Iridium Dioxide and Peroxo Iridium(VI) Dioxide in Solid Argon

Angelo Citra and Lester Andrews*

Department of Chemistry, University of Virginia, Charlottesville, Virginia 22901

Received: February 3, 1999; In Final Form: April 6, 1999

Laser-ablated iridium atoms react with O_2 to give the linear dioxide OIrO and the side-bound dioxygen adduct $(O_2)IrO_2$ as primary reaction products, with ν_3 absorptions at 930.0 and 875.0 cm^{-1}, respectively. The $(\nu_1 + \nu_3)$ combination bands for these species were observed, confirming the assignments of the ν_1 and ν_3 modes for $(O_2)IrO_2$ and providing an estimate for the ν_1 mode in OIrO. The symmetric and antisymmetric stretching modes of the $Ir(O_2)$ ring in $(O_2)IrO_2$ were also observed. Density functional calculations support these assignments and show that the $(O_2)IrO_2$ species is best formulated as a peroxide with iridium in the +6 oxidation state, providing the first example of an iridium(VI) oxo complex.

Introduction

Transition metal oxygen complexes are of interest, since they provide models for larger biological molecules.[1] They are also of interest because of their role in the oxidation of organic molecules, and finding transition metal oxo complexes that can serve as oxidizing or oxygen atom transfer agents to inert organic substrates is an important goal.[2] There are relatively few stable oxo complexes of the late transition metals because the oxo group is stabilized by highly oxidized electron-deficient metal centers. Metal−oxo (M−O) groups are stabilized at metal centers with an oxidation state of at least +4 and no more than four d electrons.[3] Excess d electrons populate molecular orbitals with M−O π^* character that destabilize the bonding. This is not easily achieved for the transition metals beyond the iron group, as it requires very high oxidation states that are usually not attainable. Even higher oxides of the form MO_3 and MO_4 are only known for d^0 metals with oxidation states of +6 and +8, examples being oxygen complexes of rhenium and osmium.[3]

Reaction of energetic transition metal atoms with oxygen and subsequent isolation of the products in an inert matrix maximizes the opportunity for metal−oxygen interaction and association to occur. In this study iridium is found to have a great affinity for oxygen, and under these experimental conditions iridium(IV) in IrO_2 is readily oxidized to iridium (VI) in $(O_2)IrO_2$. This information may prove useful in low-temperature oxidation reactions involving iridium complexes. Also, the molecular fragments and aggregates characterized in this infrared study of iridium atom chemistry will provide a means by which similar functionality may be recognized in other complexes. It also tests the effectiveness of electronic structure calculations when applied to molecules containing third-row transition metal atoms.

Experimental Section

The technique for laser ablation and FTIR matrix investigation has been described previously.[4−6] Iridium metal (Goodfellow) was mounted on a rotating (1 rpm) stainless steel rod. The Nd:YAG laser fundamental (1064 nm, 10 Hz repetition rate, 10 ns pulse width, 40−50 mJ pulses) was focused on the target through a hole in the CsI cryogenic window (maintained at 7−8 K). Metal atoms were co-deposited with 1% O_2 ($^{16}O_2$, $^{18}O_2$, $^{16,18}O_2$, and mixtures) in argon at 5−8 mmol/h for 1−2 h periods. FTIR spectra were recorded with 0.5 cm^{-1} resolution on a Nicolet 550. Matrix samples were successively warmed and recooled, and more spectra were collected; the matrix was subjected to broad-band photolysis with a medium-pressure mercury arc (Philips, 175 W) with the globe removed (240−580 nm) at different stages in the annealing cycles.

Results

Infrared spectra and density functional theory calculations of iridium−oxygen reaction products will be presented in turn. Spectra in the regions 1900−1780, 1060−860, and 700−480 cm^{-1} for $^{16}O_2$ are shown in Figures 1 and 2, respectively. The spectra obtained using isotopically scrambled oxygen are shown in Figure 3. All absorptions and isotopic counterparts are listed in Table 1.

Density functional theory (DFT) calculations using the Gaussian 94 program[7] were employed to calculate structures and frequencies for iridium oxide product molecules to verify assignments and to provide information on their ground-state properties. The BPW91 functional, D95* basis set for oxygen, and Los Alamos ECP plus DZ basis set for iridium were used for all calculations.[8−10] The nature of the bonding in the product molecules was investigated using a natural bond orbital analysis (NBO), where a localized bonding scheme is used with lone pairs and bonding pairs being the basic units of molecular structure.[11] The calculated geometries and relative energies, calculated frequencies, and NBO analyses are given in Tables 2−5, respectively.

Discussion

The major products will be identified with the help of isotopic data and DFT calculations.

IrO. Little experimental data are available on the IrO molecule. Spectroscopic constants for several excited states have been determined from electronic emission spectra, but no information is available regarding the ground state.[12] Absorption spectral studies on matrix-isolated IrO done to determine its ground state were unsuccessful.[13] The abstraction of an oxygen

10.1021/jp990388o CCC: $18.00
Published on Web 05/12/1999

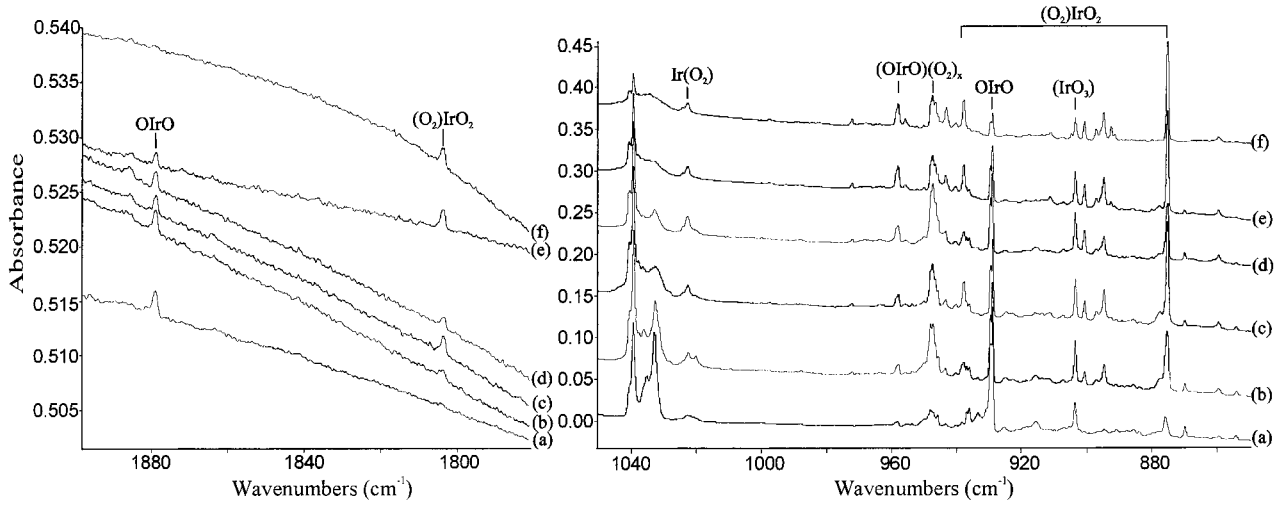

Figure 1. Infrared spectra in the 1900−1780 and 1050−850 cm^{-1} regions for laser-ablated iridium atoms co-deposited with oxygen (1%) in argon on a 7−8 K window after (a) deposition with $^{16}O_2$ for 1 h, (b) annealing to 25 K, (c) annealing to 30 K, (d) 25 min photolysis, (e) annealing to 35 K, and (f) annealing to 40 K.

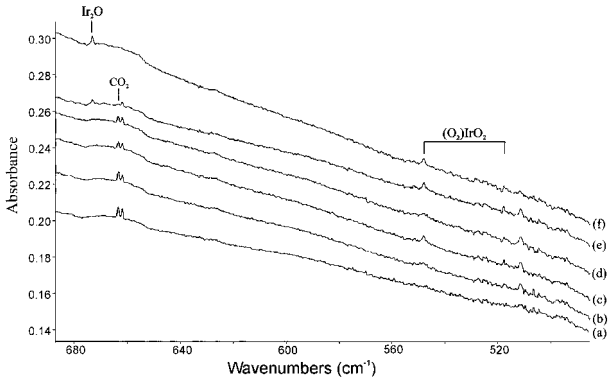

Figure 2. Infrared spectra in the 685−500 cm^{-1} region for laser-ablated iridium atoms co-deposited with oxygen (1%) in argon on a 7−8 K window after (a) deposition with $^{16}O_2$ for 1 h, (b) annealing to 25 K, (c) annealing to 30 K, (d) 25 min photolysis, (e) annealing to 35 K, and (f) annealing to 40 K.

atom from O_2 by iridium is endothermic by 87 kJ/mol, so thermally produced iridium atoms are not expected to give IrO when reacted with O_2.[14] However, laser-ablated iridium atoms should be sufficiently energetic to overcome this thermodynamic barrier. A band due to IrO should be readily distinguishable by its isotopic ratio, which is expected to be slightly less than the calculated harmonic diatomic ratio 1.055 56, and by the lack of intermediate bands in either the mixed or scrambled isotopic experiments. Unfortunately, the only band that meets these requirements is at 673.3 cm^{-1}, too low to be due to a terminal Ir−O stretching mode. This band is assigned to the cyclic Ir_2O molecule as discussed in detail below.

Both the doublet and quartet states of IrO have been calculated using DFT, and the results are summarized in Tables 2 and 3. To the best of our knowledge, no ab initio calculations have been performed for IrO, and these represent the first theoretical predictions for this molecule. The doublet and quartet optimum geometries are close in energy, but $\langle S^2 \rangle$ for the doublet state is 0.7542, indicating significant spin contamination. This makes the properties calculated for this state, including the energy, too unreliable for comparison with the quartet state or with experiment. The $\langle S^2 \rangle$ value for the quartet state is 3.7500 and so may be considered reasonable. The frequency predicted for the quartet state is 914.8 cm^{-1}, but none of the bands in this region are reasonable assignments to IrO. The molecule is almost certainly present, but the absorption may be weak and obscured by other bands. Furthermore, the low yield of IrO may be due to the almost exclusive formation of OIrO in the reaction between Ir and O_2, with IrO being only a minor product. An NBO analysis for the $^4\Sigma^-$ state of IrO predicts a double bond composed of σ and π bonds.

OIrO. An intense, sharp doublet is observed at 929.5 and 929.0 cm^{-1} on deposition. The intensities remain unchanged during photolysis but decrease during annealing. The ^{18}O counterparts for these peaks are at 884.4 and 883.8 cm^{-1}, giving isotopic 16/18 ratios of 1.051 00 and 1.051 14. The closely spaced doublets due to ^{193}Ir (61.5%) and ^{191}Ir (38.5%) in natural abundance verify the participation of a single Ir atom, and the iridium isotope ratios are 1.000 54 and 1.000 68 in the $^{16}O_2$ and $^{18}O_2$ experiments, respectively. The oxygen and iridium isotope ratios expected for the (harmonic) diatomic molecule are 1.055 61 ($^{193}Ir^{16}O/^{193}Ir^{18}O$) and 1.000 37 ($^{193}Ir^{16}O/^{191}Ir^{16}O$). The smaller oxygen and larger iridium isotopic ratios for the observed bands relative to the diatomic ratios indicate that they are due to the antisymmetric stretching mode ν_3 (σ_u for linear molecule) of OIrO. By use of the observed isotopic ratios and the appropriate **G**-matrix element, the molecule is found to be linear.[15,16]

Matrix-isolated OIrO has previously been prepared by the reaction of laser-ablated Ir with O_2, observed via ESR spectroscopy, and found to be linear along with ORhO and OCoO.[17] This result is in agreement with a qualitative Walsh type treatment of triatomic molecules, which predicts a linear geometry for transition metal triatomics with 19 valence electrons.[18] Finally, the linear ORhO molecule has been observed at 900.1 cm^{-1} in similar experiments with laser-ablated rhodium and oxygen.[19]

No intermediate peak is observed when a mixture of $^{16}O_2$ and $^{18}O_2$ is reacted, indicating that OIrO is produced by insertion of Ir into the O−O bond rather than through an IrO precursor. An intermediate peak is observed at 891.4 cm^{-1} in experiments with scrambled isotopic oxygen to give a 1:1.3:1 intensity pattern, which indicates that two equivalent oxygen atoms are involved. There are three important facts to note regarding this peak. The first is that it does not appear during annealing when only pure isotopic $^{16}O_2$ and $^{18}O_2$ are present, indicating that the addition of oxygen atoms to IrO is not occurring in the matrix even though oxygen atoms are present as shown by the small growth of ozone during early annealing. The second is the large

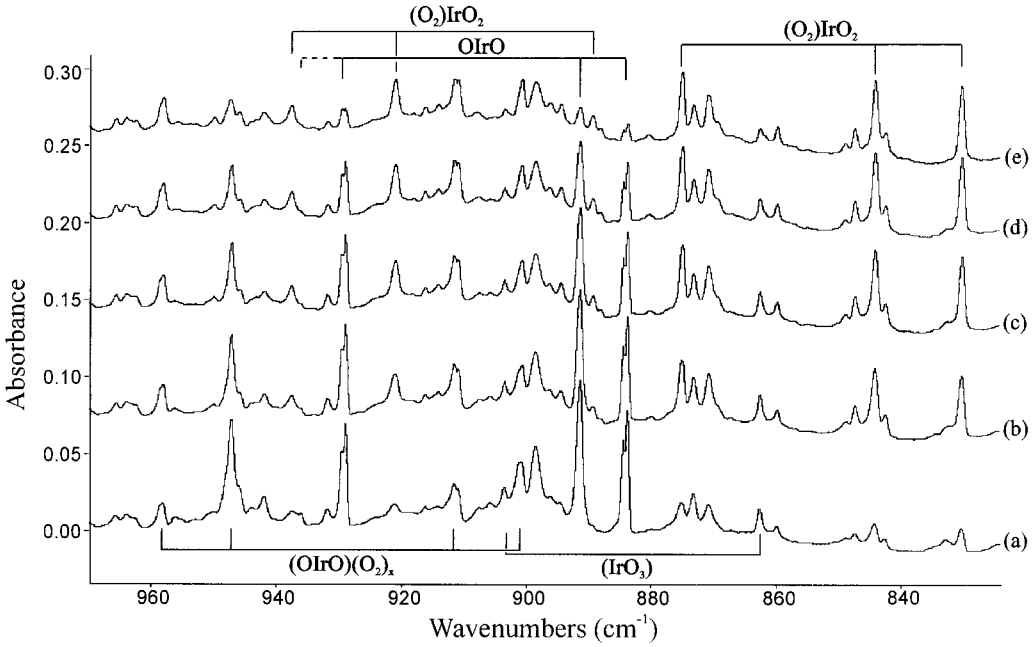

Figure 3. Infrared spectra in the 970−870 cm^{-1} region for laser-ablated iridium atoms co-deposited with $^{16}O_2 + {}^{16}O^{18}O + {}^{18}O_2$ (2%) in argon on a 7−8 K window after (a) deposition for 1 h, (b) annealing to 25 K, (c) annealing to 30 K, (d) annealing to 35 K, and (e) annealing to 40 K.

TABLE 1: Infrared Absorptions (cm^{-1}) Observed Following the Co-deposition of Laser-Ablated Iridium Atoms with Oxygen/Argon Mixtures at 7−8 K

$^{16}O_2$	$^{18}O_2$	$^{16}O_2 + {}^{18}O_2$	$^{16}O_2 + {}^{16,18}O_2 + {}^{18}O_2$	isotopic shift	assignment
1879.3	1780.7	1879.3, 1780.7	1879.3, 1837.1, 1780.7	1.055 37	OIrO
1803.8	1710.3	1803.8, 1710.3	1803.8, 1760.3, 1710.3	1.054 67	$(O_2)IrO_2$
1548.0	1460.2	1548.0, 1460.2	1548.0, 1506.7, 1460.2	1.060 13	$Ir_x(O_2)$
1533.2	1446.9	1533.2, 1446.9	1533.2, 1490.7, 1446.9	1.059 43	$Ir_x(O_2)$
1531.3	1445.4	1531.3, 1445.4	1531.3, 1489.2, 1445.4	1.059 43	$Ir_x(O_2)$
1118.7	1055.8	1118.7, 1084.8, 1055.8	1118.7, 1102.3, 1087.6, 1084.8, 1071.1, 1055.8	1.059 58	O_4^+
1111.2	1048.7	1111.2, 1048.7	1111.2, 1080.4, 1048.7	1.059 60	$Ir_x(O_2)$
1109.3	1046.6	1109.3, 1046.6	1109.3, 1078.5, 1046.6	1.059 91	$Ir_x(O_2)$
1039.3	982.1	1039.3, 1025.4, 991.4, 982.1	1039.3, 1025.4, 1016.5, 1005.9, 991.4, 982.1	1.058 24	O_3
1032.9	976.1	1032.9, 1019.4, 985.4, 976.1	1032.9, 1019.4, 1010.3, 999.6, 985.4, 976.1	1.058 19	O_3 site
1024.2	967.4	1024.2, 967.4	*a*	1.058 71	$Ir(O_2)$ site
1022.6	965.9	1022.6, 965.9	*a*	1.058 81	$Ir(O_2)$
1020.2	962.9	1020.2, 962.9	*a*	1.059 51	$Ir(O_2)$ site
958.0	911.5	958.0, 911.5	958.0, 911.5	1.051 01	$(OIrO)(O_2)_x$
947.4	900.7	947.4, 900.7	947.4, 900.7	1.051 85	$(OIrO)(O_2)_x$
937.7	888.0	937.7, 888.0	937.7, 921.0, 888.0	1.055 97	$(O_2)IrO_2$
936.9	891.2	936.9, 891.2	*a*	1.051 28	$O^{191}IrO$ site
936.2	890.5	936.2, 890.5	*a*	1.051 32	$O^{193}IrO$ site
929.5	884.4	929.5, 884.4	929.5, 929.0, 891.4	1.051 00	$O^{191}IrO$
929.0	883.8	929.0, 883.8	884.4, 883.8	1.051 14	$O^{193}IrO$
904.8	863.7	*a*	*a*	1.047 59	(IrO_3 site)
903.5	862.7	*a*	*a*	1.047 53	(IrO_3)
900.7	859.9	*a*	*a*	1.047 45	(IrO_3 site)
897.0	847.1	*a*	*a*	1.058 91	$(OIrO)(O_2)_x$
895.5	855.0	*a*	*a*	1.047 37	(IrO_3 site)
894.8	845.0	*a*	*a*	1.058 93	$(OIrO)(O_2)_x$
877.6	832.7	*b*	*b*	1.053 92	$(O_2)IrO_2$ site
875.0	830.0	875.0, 830.0	875.0, 844.2, 830.0	1.054 11	$(O_2)IrO_2$
859.4	821.0	*b*	*b*	1.046 77	?
673.3	637.6	673.3, 637.6	673.3, 637.6	1.055 99	Ir_2O
547.7	520.7	*b*	*b*	1.051 85	$(O_2)IrO_2$
517.7	489.5	*b*	*b*	1.057 61	$(O_2)IrO_2$
511.5	487.4	511.5, 487.4	511.5, 487.4	1.049 45	?

[a] Spectral region too congested to distinguish intermediate components. [b] Pure isotope bands not present in mixed/scrambled isotopic experiment.

asymmetry of the triplet in the scrambled isotopic experiment: the intermediate band is 15 cm^{-1} lower than the midpoint of the pure $^{16}O_2$ and $^{18}O_2$ bands. This asymmetry is due to interaction between the symmetric stretching ν_1 (σ_g for linear molecule) and ν_3 modes that have the same symmetry in the mixed isotopic molecule. That the observed shift is negative shows that the ν_1 mode lies higher than the ν_3 mode, and the magnitude of the shift indicates that it is close to ν_3. The ν_1 mode is infrared-inactive in the linear molecule, but if the ($\nu_1 + \nu_3$) combination band is observed, it can be used to estimate the frequency of the ν_1 mode. This is the case for OIrO; weak bands are observed at 1879.3 and 1780.7 cm^{-1} in the $^{16}O_2$ and

TABLE 2: Geometries and Relative Energies Calculated Using DFT (BPW91)

molecule	electronic state	relative energy (kJ/mol)	$\langle S^2 \rangle$	geometry (Å, deg)[a]
IrO	$^2\Pi$	+18	0.7542	r(Ir−O) 1.693
	$^4\Sigma^-$	0	3.7500	r(Ir−O) 1.742
OIrO	$^2A_1$	0	0.7500	r(Ir−O) 1.710, ∠OIrO 155.8
	$^4B_2$	+96	3.7500	r(Ir−O) 1.747, ∠OIrO 118.8
Ir(O_2)	$^2A_2$	+357	0.7500	r(Ir−O) 1.921, r(O−O) 1.388
	$^4B_1$	+457	3.7500	r(Ir−O) 2.078, r(O−O) 1.377
IrOO	$^2A'$	+375	0.7510	r(Ir−O) 1.813, r(O−O) 1.293, ∠IrOO 120.1
	$^4A''$	+440	3.7501	r(Ir−O) 1.954, r(O−O) 1.294, ∠IrOO 121.3
$(O_2)IrO_2$	$^2A_2$	+2	0.7500	r(Ir−O_t) 1.733, r(Ir−O_c) 1.938, r(O_c-O_c)1.444, ∠O_tIrO_t 110.2, ∠O_cIrO_c 43.7
	$^4A_1$	+81	3.7500	r(Ir−O_t) 1.711, r(Ir−O_c) 3.540, r(O_c-O_c) 1.238, ∠O_tIrO_t 155.9, ∠O_cIrO_c 20.1
$(OO)IrO_2$	$^2A''$	0	0.7500	r(Ir−O_t) 1.709, r(Ir−O_c) 2.028, r(O_c-O_c) 1.291, ∠O_tIrO_t 142.1, ∠Ir$O_c$$O_c$ 116.9
	$^4A'$	+82	3.7500	r(Ir−O_t) 1.743, r(Ir−O_c) 1.953, r(O_c-O_c) 1.299, ∠O_tIrO_t 115.2, ∠Ir$O_c$$O_c$ 127.2
Ir_2O	$^1A_1$	+16		r(Ir−O) 1.816, r(Ir−Ir) 2.568, ∠IrOIr 90.0
	$^3A_2$	0	2.0000	r(Ir−O) 1.869, r(Ir−Ir) 2.498, ∠IrOIr 83.9
	$^5A_2$	+91	6.0000	r(Ir−O) 1.833, r(Ir−Ir) 3.345, ∠IrOIr 131.8
Ir_2O_2	^1A_g	+14		r(Ir−O) 1.899, pIrOIr 97.4, d(OIrIrO) 180.0
	$^3B_{2u}$	0	2.0030	r(Ir−O) 1.903, ∠IrOIr 100.6, d(OIrIrO) 180.0
	^5A_g	+49	6.0087	r(Ir−O) 1.944, ∠IrOIr 86.3, d(OIrIrO) 180.0

[a] O_t and O_c denote terminal and cyclic oxygen atoms.

TABLE 3: Frequencies Calculated for Selected Geometries

molecule (electronic state)	frequencies (cm^{-1}); intensities (km/mol)
IrO ($^4\Sigma^-$)	914.8 (31)
OIrO ($^2A_1$)	997.5 (4), 988.4 (189), 86.7 (7)
Ir(O_2) ($^2A_2$)	1020.4 (47), 576.8 (2), 393.5 (8)
$(O_2)IrO_2$ ($^2A_2$)	955.6 (76), 951.8 (5), 883.4 (100), 550.6 (4), 467.8 (2)
Ir_2O ($^1A_1$)	748.8 (55), 658.7 (17), 183.4 (2)
Ir_2O ($^3A_2$)	729.8 (41), 465.4 (0), 198.5 (1)
Ir_2O_2 (^1A_g)	666.9 (0), 582.1 (12), 507.5 (0), 431.2 (60), 240.3 (15), 190.6 (0)
Ir_2O_2 ($^3B_{2u}$)	651.5 (0), 618.1 (32), 547.9 (72), 464.2 (0), 207.9 (0), 37.9 (15)

TABLE 4: NBO Bonding Analysis for Iridium Oxide Products

molecule	bond[a]	population[c]	%Ir[c]	%6s[d]	%6p[d]	%5d[d]
IrO($^4\Sigma^-$) (α electrons)	Ir−O	1.00 (0.01)	34.5	47.2	1.1	51.7
IrO($^4\Sigma^-$) (β electrons)	Ir−O	1.00 (0.00)	45.2	0.0	0.3	99.7
	Ir−O	1.00 (0.00)	45.2	0.0	0.3	99.7
	Ir−O	1.00 (0.01)	33.1	45.8	0.8	53.4
OIrO (α electrons)	Ir−O_1	0.94 (0.18)	31.3	30.2	1.8	68.0
	Ir−O_2	0.94 (0.18)	31.3	30.2	1.8	68.0
	Ir−O_2	1.00 (0.26)	37.6	30.2	0.8	99.2
OIrO (β electrons)	Ir−O_2	1.00 (0.22)	29.1	4.7	0.2	95.1
	Ir−O_2	1.00 (0.26)	36.3	0.0	0.7	99.3
	Ir−O_2	1.00 (0.22)	36.3	2.1	0.6	97.3
$(O_2)IrO_2$ (α electrons)	Ir−O_1	0.96 (0.22)	35.9	23.9	0.1	76.0
	Ir−O_2	0.96 (0.22)	35.9	23.9	0.1	76.0
	Ir−Ot_1	0.99 (0.17)	37.5	22.2	0.2	77.6
	Ir−Ot_2	0.99 (0.17)	37.5	22.2	0.2	77.6
	O_1−O_2	1.00 (0.00)	0.0	0.0	0.0	0.0
$(O_2)IrO_2$ (β electrons)	Ir−O_1	0.88 (0.17)	22.4	18.1	19.0	63.0
	Ir−O_2	0.88 (0.17)	22.4	18.1	19.0	63.0
	Ir−Ot_1	0.99 (0.17)	37.2	22.5	0.2	77.4
	Ir−Ot_1	0.86 (0.19)	30.7	0.0	35.3	64.7
	Ir−Ot_1	0.87 (0.20)	17.1	3.8	19.7	76.5
	Ir−Ot_2	0.92 (0.11)	28.8	30.0	4.8	65.1
	Ir−Ot_2	0.86 (0.19)	30.7	0.0	35.3	64.7
	O_1−O_2	1.00 (0.00)	0.0	0.0	0.0	0.0
Ir_2O (α electrons)	Ir_1−O	1.00 (0.08)	30.5	33.2	0.3	66.5
	Ir_2−O	1.00 (0.08)	30.5	33.2	0.3	66.5
	Ir_1−Ir_2	0.96 (0.02)	50.0	44.3	0.4	55.3
Ir_2O (β electrons)	Ir_1−O	0.99 (0.08)	30.2	29.9	0.2	69.9
	Ir_2−O	0.99 (0.08)	30.2	29.9	0.2	69.9
	Ir_1−Ir_2	1.00 (0.00)	50.0	0.0	0.1	99.9
	Ir_1−Ir_2	1.00 (0.31)	50.0	0.0	0.0	100.0
	Ir_1−Ir_2	0.96 (0.02)	50.0	59.4	0.3	40.4
Ir(O_2) (α electrons)	Ir−O_1	0.97 (0.04)	28.5	35.0	0.1	64.9
	Ir−O_2	0.97 (0.04)	28.5	35.0	0.1	64.9
	O_1−O_2	1.00 (0.00)	0.0	0.0	0.0	0.0
Ir(O_2) (β electrons)	Ir−O_1	0.97 (0.03)	28.0	33.9	0.1	66.0
	Ir−O_1	1.00 (0.19)	24.9	0.0	0.6	99.4
	Ir−O_2	0.97 (0.03)	28.0	33.9	0.1	66.0
	O_1−O_2	1.00 (0.00)	0.0	0.0	0.0	0.0

[a] Subscript t denotes a terminal Ir−O bond. [b] The number in parentheses is the population of the corresponding antibond. [c] The total contribution of iridium orbitals to the bond. [d] Hybridization of the bond at iridium.

$^{18}O_2$ experiments, respectively. These bands show the same changes in intensity as the 929.5, 929.0 and 884.4, 883.8 cm^{-1} bands during annealing, and the isotopic ratio of 1.055 37 is within 0.1% of the value expected from the mean of the ν_1 and ν_3 isotopic ratios in the (harmonic) linear molecule. Allowing 10 cm^{-1} for anharmonicity, ν_1 is estimated at 960 cm^{-1}, only slightly higher than ν_3, as expected from the highly distorted mixed isotopic triplet. Finally, a molecule with two equivalent oxygen atoms is expected to give a 1:2:1 intensity pattern in the scrambled isotopic experiment. The reduced intensity of the central component is due to the strong coupling between the "symmetric" and "antisymmetric" modes that allows the former mode to steal intensity from the latter mode in $^{16}OIr^{18}O$. Thus, the ν_1 mode of the mixed isotopic molecule has nonzero intensity, and although the spectrum is congested, the weak 956.3 cm^{-1} band is appropriate. For the $^{16}OIr^{18}O$ molecule, the sum (891.4 + 956.3 = 1847.7 cm^{-1}) less 10 cm^{-1} for anharmonicity is in agreement with the observed 1837.1 cm^{-1} band. Finally, this strong coupling also explains the lack of iridium isotopic structure in the scrambled band. The central atom does not move in the symmetric stretch of a linear triatomic molecule, so mixing this mode with the ν_3 mode of OIrO reduces the participation by iridium relative to the pure ν_3 mode. All of the above experimental evidence confirms the matrix infrared identification of OIrO.

DFT (BPW91) calculations have been done to test the theory and predict geometry and frequencies for OIrO in both doublet and quartet states. The optimized geometries and frequencies are listed in Tables 2 and 3. The quartet state was found to lie 96 kJ/mol higher than the doublet state, and so frequencies were not calculated. This is consistent with the results of ESR

TABLE 5: Natural Orbital Populations and Charges of Iridium Oxide Products Using the D95* Basis Set on Oxygen

	iridium orbital populations			oxygen orbital populations		natural charge	
molecule	6s	5d	6p	2s	2p	q_{Ir}	q_o
IrO	1.36	7.18	0.05	1.92	4.47	+0.41	−0.41
OIrO	0.67	7.28	0.4	1.91	4.57	+1.0	−0.5
Ir_2O	0.86	7.84	0.03	1.89	4.63	+0.27	−0.54
$Ir(O_2)$	0.82	7.74	0.01	1.85	4.33	+0.41	−0.20

	iridium orbital populations			ring oxygen populations		terminal oxygen populations	
	6s	5d	6p	2s	2p	2s	2p
$(O_2)IrO_2$	0.50	6.97	0.03	1.88	4.37	1.92	4.53
		natural charge: +1.50		natural charge: −0.28		natural charge: −0.47	

TABLE 6: Geometries and Frequencies Calculated for IrO_2 and $(O_2)IrO_2$ Using the 6-311+G(3d) Basis Set on Oxygen

molecule	electronic state	$\langle S^2 \rangle$	geometry (Å, deg)[a]	frequencies (intensities)	Mulliken populations
OIrO	$^2\Sigma_g^+$	0.7500	r(Ir−O): 1.724	983.4 (0)	Ir: +1.66
			∠OIrO: 180.0	957.3 (236)	O: −0.83
$(O_2)IrO_2$	$^2A_2$	0.7500	r(Ir−O_t): 1.738	946.9 (89)	Ir: +2.55
			r(Ir−O_c): 1.938	938.8 (1)	O_t: −0.82
			r(O_c-O_c): 1.445	880.2 (115)	O_c: −0.45
			∠O_tIrO_t: 109.7	568.9 (4)	
			∠O_cIrO_c: 43.7	500.4 (3)	

[a] O_t and O_c denote terminal and cyclic oxygen atoms.

spectroscopy, which showed the molecule to have a doublet ground state.[17]

Our BPW91 calculations reproduce the experimental results reasonably well. The molecule has a doublet ground state, is almost linear, and the harmonic ν_1 and ν_3 modes are predicted to be 997.5 and 988.4 cm^{-1}. The scale factors (observed/calculated) are 0.96 and 0.94, respectively, which are lower than scale factors for pure DFT functionals and the ECP and other first-row transition metal compounds.[20]

The calculated Ir−O bond lengths are in the range 1.6−1.8 Å expected for metal−oxo bonds with multiple bond character.[3] The formal oxidation state of iridium is +4, but the atomic charges derived from the Mulliken population analysis are only +0.91 and −0.45 at iridium and oxygen, respectively, much lower than their formal charges.

Examination of the natural bond orbitals indicates that each Ir−O bond can be formulated as one Ir−O σ bond and one-half π bond, both polarized toward the oxygen atom. It is clear from the bonding analyses that the Ir(5d) orbitals dominate the metal contribution to the bonding. This is consistent with the results of a previous theoretical study of the bonding in oxo and nitride complexes, where the metal−ligand bonding for second- and third-row transition metals was found to be dominated at the metal by contributions from the d orbitals.[21]

To test the basis set effects, OIrO was recalculated using the larger 6-311+G(3d) basis set on oxygen, which includes diffuse functions and three sets of d polarization functions. The results of these calculations are summarized in Table 6; OIrO is calculated to be linear with a $^2\Sigma_g^+$ ground state, in complete agreement with the ESR study of this molecule.[17] This shows that the bent geometry calculated earlier was a consequence of the small basis set rather than the theoretical method used. The ν_1 and ν_3 frequencies are calculated to be 983.4 and 957.3 cm^{-1}, respectively, in closer agreement with experimental values (scale factors are 0.98 and 0.97). The Mulliken charges are +1.66 and −0.83 for iridium and oxygen, larger than with the smaller basis set. Using the larger basis set is expected to improve the charge distribution in the molecule, and these charges are probably more realistic than those calculated using the smaller basis set.

$(O_2)IrO_2$. A sharp peak is observed at 875.0 cm^{-1} after deposition with approximately one-sixth the intensity of the 929.5, 929.0 cm^{-1} doublet. Annealing increases the band markedly, and photolysis decreases the band by a factor of 2. Other peaks at 937.7, 548.0, and 517.7 cm^{-1} track with this band under all conditions of annealing and photolysis, as does a weak band at 1803.8 cm^{-1}. Isotopic counterparts for these bands lie at 830.0, 888.0, 520.7, 517.7, and 1710.3 cm^{-1}. The low-frequency bands are too weak to be seen in the mixed and scrambled experiments, but the three higher frequency bands show intermediate components in experiments with scrambled oxygen at 1760.3, 921.0, and 844.2 cm^{-1}. These intermediate mixed isotopic bands are not present on deposition in the mixed $^{16}O_2$ + $^{18}O_2$ isotopic experiment but grow in slightly on annealing.

Given the abundance of OIrO and O_2 in the matrix, it is reasonable to expect complexation of the primary reaction product with oxygen. This behavior is observed for other metal−oxygen systems including cobalt,[6] vanadium, niobium, and tantalum.[22,23] In the Co system the complexing oxygen molecule was bound to the metal end-on, but sideways binding was also thought to be present. With V, Nb, and Ta, sideways complexing of O_2 to the bent dioxide molecule has been observed and supported by DFT calculations. In the case of iridium the dominant form of complexation of OIrO by O_2 is through a side-on approach to give a species of C_{2v} symmetry. The 875.0 cm^{-1} band corresponds to the antisymmetric stretching mode of the OIrO unit (b_1 symmetry in the C_{2v} point group). Its isotopic ratio can be used to estimate the bond angle in the OIrO unit (as in the case of a triatomic molecule), and this gives a value of 108°. In the case of the structurally analogous species CrO_2Br_2 and CrO_2Cl_2, it was found that the Cr isotope ratios for the b_1 Cr−O stretching mode gave an *upper* limit for the OCrO angle rather than the lower limit, as is usually the case for the central atom.[24] The 937.7 cm^{-1} band is assigned to the OIrO symmetric stretching mode.

Another estimate for the OIrO bond angle can be derived from the measured intensities of the bands using the bond dipole approximation.[15,25] As discussed above, the 937.7 cm^{-1} band is assigned to the symmetric (a_1) Ir−O stretching mode, which is largely uncoupled to the Ir(O_2) symmetric stretch and the O−O stretching mode that have the same symmetry. Four sets of intensity data from spectra recorded after annealing experi-

ments have been used in this model, and the average bond angle is found to be 109°, with only a 2° spread about the mean. This is in excellent agreement with the value determined from the isotopic data for the ν_3 mode of the OIrO unit. These results clearly indicate that the OIrO molecule is significantly distorted from linearity when bound to dioxygen.

The low-frequency bands at 548.0 and 517.7 cm^{-1} ($^{16}O_2$) are due to the symmetric and antisymmetric stretching modes in the cyclic Ir(O_2) unit. Which band corresponds to each mode can be determined from their isotopic ratios. In the case of a triatomic molecule with an acute angle, the ν_1 mode is expected to demonstrate an isotopic ratio for the outer atoms *less* than the diatomic ratio. Conversely, the ν_3 mode will show a greater isotopic ratio than the diatomic molecule. The isotopic ratios for the two bands of 1.052 43 and 1.057 61 show that the bands correspond to the symmetric and antisymmetric modes of the Ir(O_2) unit, respectively.

The assignment of the 875.0 and 937.7 cm^{-1} bands to the same molecule is supported by the combination band observed at 1803.8 cm^{-1}, which tracks with the fundamentals under all conditions. The sum of the fundamentals is 1812.7 cm^{-1}, the difference of 8.9 cm^{-1} arising from anharmonicity. The observation of the $\nu_1 + \nu_3$ combination band for (O_2)IrO_2 is expected, since the analogous mode was also observed for OIrO.

This discussion supports the assignment of these bands to the side-bound complex (O_2)IrO_2. If the incoming oxygen molecule were bound to OIrO in an end-on fashion, only one low-frequency Ir−O stretching mode would be present, so the side-bound complex (O_2)IrO_2 is the better assignment. The fact that the scrambled intermediate peak at 844.2 cm^{-1} for the ν_3 mode has the same intensity deficit observed for OIrO is further evidence that the species under consideration is derived from that molecule. In this case, the symmetric stretch at 921.0 cm^{-1} is more intense and the sum 844.2 + 921.0 = 1765.2 cm^{-1} is 4.9 cm^{-1} higher than the combination band observed at 1760.3 cm^{-1}.

As noted above, the pure isotope bands associated with this molecule show large *decreases* on photolysis. However, the intermediate bands at 1760.3, 921.0, and 844.2 cm^{-1} in the mixed isotopic experiment reveal an unmistakable *increase* on photolysis. This must be due to a photoinduced scrambling of the oxygen atoms in the mixed isotopic molecules ($^{16}O_2$)$Ir^{18}O_2$ and ($^{18}O_2$)$Ir^{16}O_2$ involving breaking and then re-forming the O−O bond.

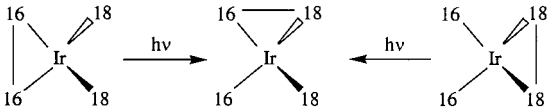

This shows that iridium cannot support an oxidation state higher than +6, since the IrO_4 species containing four terminal Ir−O bonds that is initially formed on photolysis of the O−O bond is not stable even in the cold inert matrix; it simply re-forms the peroxide complex. This is in contrast to the OsO_4 molecule, which has four oxo groups and osmium in the +8 oxidation state. The sensitivity of (O_2)IrO_2 to photolysis is consistent with the fact that many neutral iridium peroxo complexes lose O_2 on irradiation.[26]

DFT was used to investigate the binding of O_2 to OIrO. Both the side-on and end-on configurations were investigated in both doublet and quartet states, and the results are summarized in Table 2. The doublet states for each geometry minimize the energy of the complex, the side-on and end-on bound geometries being almost identical in energy. As was discussed above, the end-on configuration is incompatible with experimental results and is rejected in favor of the side-on geometry. The binding energy of O_2 to OIrO in (O_2)IrO_2 is calculated to be 68 kJ/mol including zero-point energy corrections but neglecting BSSE. The accuracy of this binding energy is unknown, but there is no doubt that the sign is correct and that complex formation is a spontaneous process. The fact that the addition reaction occurs readily on annealing suggests that little or no activation energy is required, not unexpected for the combination of two open-shell species. The most striking result is the bond angle calculated for the (O_2)IrO_2 complex, which is significantly distorted from that in the uncomplexed linear OIrO molecule. The calculated value of 110.2° is in excellent agreement with the experimental values derived earlier. The stretching frequencies calculated using the BPW91 structures are shown in Table 3 (bending frequencies excluded).

The calculated frequencies lend support to the assignment of the observed bands to the (O_2)IrO_2 complex. The most intense band is predicted to be the antisymmetric Ir−O stretch in the OIrO unit, and the calculated value is within 8.4 cm^{-1} of the experimental value. The calculated Ir(O_2) stretching modes are also compatible with experimental results: the intensities are very low and are nearly equal, the frequencies are in good agreement with the measured values, and the symmetric Ir(O_2) stretch is predicted to lie at higher frequency than the asymmetric mode.

Only one of the two high-frequency a_1 modes is predicted to have appreciable intensity, 76% that of the b_1 mode, and is principally the O−O stretching mode with a large contribution from the OIrO symmetric stretching mode. The other a_1 mode is principally the OIrO symmetric stretch and is predicted to have a very similar frequency but only low intensity. This is in poor agreement with experimental results. Although the agreement between the calculated 955.6 cm^{-1} and experimental 937.7 cm^{-1} bands is good, the isotopic ratio of 1.055 99 is too low for an O−O stretching mode. Also, the measured intensity for the 937.7 cm^{-1} band is only 34 km/mol on the same scale by which the 875.0 cm^{-1} band has an intensity of 100 km/mol. This disagreement has arisen because DFT has overestimated the coupling between the a_1 O−O and the OIrO stretching modes. If the modes were really so strongly coupled, the observed splitting patterns in the mixed and scrambled isotope experiments would be different from those actually observed. A quartet of equal intensity peaks would be present in the mixed experiment due to ($^{16}O_2$)$Ir^{16}O_2$, ($^{16}O_2$)$Ir^{18}O_2$, ($^{18}O_2$)$Ir^{16}O_2$, and ($^{18}O_2$)$Ir^{18}O_2$, and a triplet of triplets would be present in the scrambled experiment. Instead, a simple 1:2:1 triplet asymmetric toward the high-frequency side is observed in the scrambled spectrum, and no intermediate is initially present in the mixed experiment. This and the relatively low isotopic ratio indicate that the observed band corresponds to a mode that is predominantly the OIrO symmetric stretching mode and not the O−O stretching mode as predicted by theory. The excessive coupling that is predicted throws off the intensities, erroneously adding intensity to the O−O stretching mode and removing it from the OIrO ν_1 mode.

The Mulliken charges calculated for (O_2)IrO_2 using BPW91 are +1.34, −0.43, and −0.24 for iridium, the oxygens in the OIrO subunit, and the oxygens in O_2 respectively. Recall the values of +0.91 and −0.45 calculated for OIrO using the same method. If a charge of −0.45 on the terminal oxygens is interpreted as representing a formal oxidation state of −2, then the O_2 unit in the complex is best described as being the peroxide O_2^{2-} and the central iridium atom as formally being

in oxidation state +6. The O−O bond length and frequency are also indicators of the charge on the O_2 unit and may be used to determine whether it should be described as a peroxide (O_2^{2-}) or superoxide (O_2^-). The calculated O−O bond length of 1.444 Å is shorter than 1.48 and 1.49 Å known for H_2O_2 and O_2^{2-} but is in the range 1.4−1.5 Å expected for a peroxo ligand. It is outside the 1.1−1.3 Å range expected for a superoxo ligand. Similarly, the vibrational frequency of 955.6 cm^{-1} is just beyond the high-frequency end of the range expected for a peroxo group (790−930 cm^{-1}) but is further outside the range expected for a superoxo ligand (1075−1195 cm^{-1}).[27] Of course, the accuracy of the calculated frequency is unknown, since this mode was not observed, but the frequencies of the observed modes suggest an error of only a few tens of wavenumbers. Bond lengths in transition metal compounds can be calculated to within 0.05 Å, if not better.[28] The bond length in free O_2 calculated using the same method and basis set is 1.236 Å, longer than the experimental value of 1.208 Å by only 0.028 Å. Considering these relatively small margins for error in the calculated frequency and bond length, the O_2 unit in $(O_2)IrO_2$ is best described as a peroxo ligand. The Ir−O bond lengths of 1.938 Å are shorter than Ir−O single bond lengths of 2.035 and 2.04 Å observed in $Cp^*_2Ir_2(O)(PMe_3)$[29] and $Ir_2I_2(CO)_2(\mu\text{-}O_2)(dppm)_2$,[30] and so it is reasonable to regard the $Ir(O_2)$ unit as consisting of three bonds each with a bond order of at least 1. Single bonds to a metal by oxygen are usually 0.2−0.4 Å longer than metal−oxo bonds,[3] the calculations for iridium being in the lower half of this range. Designating the dioxygen group as a peroxide is consistent with the fact that most known iridium dioxgyen complexes are peroxides.[31]

An NBO analysis was performed on this species to give more insight into the bonding of $(O_2)IrO_2$, and the results are consistent with the above discussion. The natural charges for $(O_2)IrO_2$ and OIrO can be used to show that the O_2 subunit is best described as a peroxo group, just as was found using the Mulliken charges. The terminal Ir−O bonds are σ bonds with additional π bonding, and the bonds between iridium and dioxygen atoms are essentially single σ bonds. The O−O bond is also a single σ bond, as expected for a peroxo group. The iridium 5d orbitals dominate the bonding at the metal atom, as was found for OIrO. However, the iridium 6p orbitals contribute significantly to the Ir−O π bonds in the complex, whereas the metal contribution to these bonds in OIrO was almost exclusively from the 5d orbitals (>99%).

The calculation for $(O_2)IrO_2$ was repeated using the 6-311+G(3d) basis set for oxygen, and the results are summarized in Table 6. The ground state is unchanged, $^2A_2$, and the optimized geometry is almost identical to that obtained using the smaller basis set. The calculated frequencies are in better agreement with experimental results, though the symmetric Ir−O and the O−O stretching modes are still erroneously predicted to be strongly coupled, the latter mode having an anomalously high intensity. The Mulliken charges are calculated to be +2.55, −0.82, and −0.45 for iridium and the terminal and cyclic oxygen atoms, respectively, considerably larger than with the smaller basis. However, the relationship between the atomic charges in OIrO and $(O_2)IrO_2$ is unchanged with the larger basis set. Finally, the energy change for the addition of O_2 to OIrO is calculated to be −125 kJ/mol, almost double the value calculated using the smaller basis set on oxygen. These results show that using the larger basis set gives frequencies in better agreement with experimental results and gives significant improvements in the charge distributions and binding energy. However, the molecular parameters calculated for OIrO and $(O_2)IrO_2$ using the smaller basis set are adequate in determining the extent of the interaction between OIrO and O_2.

Iridium(VI) has been observed for several ionic iridium perovskites including Sr_2MgIrO_6 and Sr_2CaIrO_6,[32] but this is the first example of an iridium(VI) oxo complex, which is formed readily from the dioxide at low temperatures. Up until now IrF_6 is the only known Ir(VI) complex.

$(OIrO)(O_2)_x$. Several other dioxygen complexes of OIrO are present in the matrix in addition to the primary complex. Of these, the most prominent complex absorbs at 947.4 cm^{-1}. This band is weak initially, grows strongly on early annealing but then decreases at higher temperatures. The band shows moderate growth on photolysis. The $^{18}O_2$ counterpart for this band is at 900.7 cm^{-1}, giving a ratio of 1.051 85, indicative of an antisymmetric mode in an OIrO unit. No intermediate bands are observed in the mixed isotope experiment, just as was found for OIrO. However, no intermediate band is apparent in the scrambled isotopic experiment either, and this would seem to invalidate the assignment of the band to an OIrO species. However, the intensity of the $^{16}O_2$ peak is much greater than the $^{18}O_2$ peak in the scrambled experiment, even though $^{16}O_2$ and $^{18}O_2$ are known to be present in equal abundance. This peculiarity can be explained if the scrambled band due to the mixed isotopic molecule $(^{16}OIr^{18}O)(O_2)_x$ is on top of the pure $^{16}O_2$ band. This can occur if the ν_3 mode lies slightly higher than the ν_1 mode in this complex, causing a sufficiently large asymmetry in the scrambled isotopic triplet such that the intermediate band eclipses the pure $^{16}O_2$ band, giving rise to an anomalously high intensity. The structure of this species is unknown; all that can be determined is that the 947.4 cm^{-1} band is due to oxygen-perturbed OIrO. Bands due to other weakly perturbed OIrO species are included in Table 1.

Ir_2O. A sharp weak band grows in during annealing at 673.3 cm^{-1} with an ^{18}O counterpart at 637.6 cm^{-1}. No intermediate peaks are observed in either the mixed or scrambled isotopic experiment nor is there evidence of any secondary isotope effect in those experiments. The isotopic ratio for these bands is 1.055 99, marginally higher than the harmonic diatomic ratio of 1.055 56. IrO is predicted to absorb at a much higher frequency, and so this band cannot be assigned to the diatomic molecule. The most logical assignment is to the triatomic molecule Ir_2O. The bond angle can be estimated using the isotopic ratio; if the 673.3 cm^{-1} band is due to the ν_1 mode, then the bond angle is 85°, but if it is due to the ν_3 mode, then the angle is 95°.

DFT has been used to calculate Ir_2O, and the results are summarized in Tables 2 and 3. The singlet and triplet states are very close in energy, and both must be considered as a possible assignment to the observed band. The quintet state is higher in energy and is outside a reasonable margin for error in the calculated energies. The frequencies calculated for the singlet state are incompatible with the experimental observations, since the intensities of the ν_1 and ν_3 modes are predicted to be in an approximate 3:1 ratio. If one of the modes is observed, then the other should also be apparent, but this is not the case. The frequencies calculated for the triplet state are in very good agreement with experimental results, as only the ν_1 mode is predicted to have appreciable intensity. The error in the calculation is +56.5 cm^{-1}, almost the same error as was observed for OIrO. Finally, the calculated bond angle of 84.9° is in excellent agreement with the value of 85° expected if the observed band is interpreted as the ν_1 mode. In summary, the DFT calculations support the assignment to the ν_1 mode of cyclic Ir_2O in a triplet state.

The Ir−Ir bond length of 2.498 Å for the $^3A_2$ state is short compared to that in other diiridium species. The Ir−Ir bond lengths of 2.705 and 2.617 Å in $[Ir_2I_2(CO)_2(\mu\text{-}O_2)(dppm)_2]$[30] and $Cp^*_2Ir_2(PPh_3)(\mu\text{-}O)$[29] were interpreted as single bonds, and so the metal−metal bond in Ir_2O is expected to have a bond order greater than 1. The calculated metal−metal bond length is comparable to the value of 2.55 Å determined for the diphenylphosphido-bridged dimer $(Ph_3P)(CO)Ir(\mu\text{-}PPh_2)_2Ir(CO)(PPh_3)$ in which the metal−metal bond was interpreted as having a formal bond order of 2.[33,34]

The NBO analysis for Ir_2O shows the molecule to be composed of two single Ir−O bonds and an Ir−Ir double bond, supporting the earlier bonding analysis for the bridged dimer complex.[33,34] The oxygen orbitals in the Ir−O bonds are sp^2-hybridized with the O(2p) contribution greater than 90%, and these bonds may be designated as σ bonds that are polarized toward oxygen. The NBO analysis for the Ir−Ir bonds gave a mixture of σ, π, and δ bonds, each natural bonding orbital having contributions from more than one of these types. The bonding at the metal centers is dominated by the 5d orbitals, as was found for OIrO.

The rhombic ring Ir_2O_2 was also considered for assignment to the 673.3 cm^{-1} band, the diatomic isotopic ratio being as expected for this molecule. This molecule would also be expected to give a 1:2:1 intensity triplet in the scrambled isotopic experiment, but this may be absent if the large iridium masses cause the motion of the oxygen atoms to become uncoupled. The Ir_2O_2 molecule was calculated using DFT to explore this possibility, and the results are summarized in Tables 2 and 3. The molecule is predicted to be planar for the three spin states calculated, the singlet and triplet states lying very close in energy. The frequencies for these states were calculated for $Ir_2{}^{16}O_2$, $Ir_2{}^{18}O_2$, and $Ir_2{}^{16,18}O_2$. In each case the mixed isotopic molecule does not exhibit any unusual coupling effects, and so there is no way to rationalize the lack of an intermediate component in the scrambled isotopic experiments. The calculated frequencies and relative intensities are also in very poor agreement with experimental results, and the assignment of the 673.3 cm^{-1} band to Ir_2O_2 may also be rejected on those grounds.

$Ir(O_2)$. A broad band was observed at 1022.7 cm^{-1} with matrix sites at 1024.2 and 1020.2 cm^{-1} that grows on photolysis and early annealing but then decreases at higher temperature. The $^{18}O_2$ counterparts for these bands are at 965.9, 967.4, and 962.9 cm^{-1}, giving an isotopic ratio of 1.058 81 for the primary site, a typical value for an O−O stretching mode. The most reasonable assignment for this band is to $Ir(O_2)$. Such species have been observed for numerous transition metals including the platinum group metals.[34] No intermediate band is observed in the mixed isotopic experiment, which shows that only one O_2 molecule is involved. The scrambled isotopic experiment should have an intermediate component giving a 1:2:1 intensity pattern, but unfortunately, this region of the spectrum is completely obscured by ozone absorptions present in all isotopic combinations.

The $Ir(O_2)$ complex has been calculated in doublet and quartet states using DFT from both side-on and end-on (IrOO) initial geometries, and the results are summarized in Tables 2 and 3. Minima are found for both orientations, though the IrOO geometry could not be converged within the "tight" regime. The doublet states are found to be the most favorable, the side-on configuration being lower in energy than the end-on geometry by 18 kJ/mol. This is within the margin for error expected for these calculations, and so the end-on geometry cannot be rejected on this basis alone. However, reference to $(O_2)IrO_2$ strongly suggests that $Ir(O_2)$ is the correct geometry. The O−O stretching frequency predicted for $Ir(O_2)$ is 1020.4 cm^{-1}, almost equal to the experimental value. Such good agreement may have arisen through a fortunate cancellation of errors but is very encouraging nevertheless.

The NBO analysis for $Ir(O_2)$ shows that the Ir−O and O−O bonds are σ bonds, with half an Ir−O π bond shared between the two Ir−O bonds. As before, the iridium 5d orbitals dominate the bonding at the metal atom. The O−O bond is formed from sp hybrid orbitals on the oxygen atoms with over 90% p orbital character. The single σ bond between the oxygen atoms and the lack of O−O π bonding suggest that $Ir(O_2)$ should be designated as iridium(II) peroxide. Consideration of the atomic charges (either Mulliken or natural charges), as was done for $(O_2)IrO_2$, also supports this description.

IrO_3. A sharp but weak band is observed at 903.6 cm^{-1} on deposition. It shows slight growth during early annealing cycles but decreases at higher temperatures and is not affected by photolysis. The $^{18}O_2$ counterpart for this band is at 862.6 cm^{-1}, giving an isotopic ratio of 1.047 53. This is anomalously low, considering that the observed ratio for the ν_3 mode of linear OIrO is 1.051, representing the lower limit for the triatomic molecule. This region of the spectrum is congested, and no intermediate peaks can be positively identified in either the mixed or scrambled isotopic experiments. It is impossible to reconcile the low ratio with a species derived from OIrO, and a different species must be considered. A good alternative is IrO_3, with three terminal Ir−O bonds. By use of the **G**-matrix element for the degenerate stretching mode, the isotopic ratio as a function of bond angle can be calculated.[15] The lowest ratio, 1.053 40, occurs for the trigonal-planar IrO_3 molecule. This is still too high, but the neglect of the interaction between the degenerate bending and stretching modes in the calculation can account for this discrepancy. Although this is a reasonable assignment, the absence of mixed or scrambled isotopic data make it tentative. If this assignment to IrO_3 is correct, this would be another example of an Ir(VI) complex. It is reasonable that IrO_3 be present in the matrix, as the reaction of IrO_3 with oxygen atoms would explain the growth of the scrambled isotopic bands for $(O_2)IrO_2$ at 1760.3, 921.0, and 844.2 cm^{-1} in the mixed isotopic experiment during annealing.

Conclusions

Laser-ablated iridium atoms were reacted with dioxygen, and several important molecules can be identified including OIrO, $(O_2)IrO_2$, Ir_2O, and $Ir(O_2)$. The strong insertion product OIrO was characterized by iridium and oxygen isotopic splittings, and these isotopic shifts showed OIrO to be linear, in agreement with results of a previous ESR study of the molecule.[17] The geometry and frequencies for OIrO were calculated accurately with 0.96 and 0.94 scale factors using DFT (BPW91) and the D95* basis set. The calculated ν_1 and ν_3 ordering and spacing are in very good agreement with experimental results. This species is readily complexed by O_2 to give the side-on bound species $(O_2)IrO_2$, which distorts the molecule significantly from linearity, and both the ν_1 and ν_3 modes are observed. The OIrO bond angle is estimated to be 108° using the isotopic ratio for the ν_3 mode and the measured intensities of the Ir−O stretching modes. DFT calculations on this species suggest the species is best described as a peroxide, with iridium in the +6 oxidation state, higher than has previously been observed in oxygen-containing iridium complexes. Photolysis of this complex breaks and then re-forms the O−O bond, as demonstrated by the formation of $(^{16}O^{18}O)Ir^{16}O^{18}O$ from $(^{16}O_2)Ir^{18}O_2$ and $(^{18}O_2)$-

$Ir^{16}O_2$. Numerous other complexed or perturbed $(OIrO)(O_2)_x$ species are also evident, thought their exact nature cannot be determined.

The DFT (BPW91) calculations proved to be very effective in reproducing experimental results and aiding interpretation of the spectra. How accurate can we expect these calculations to be for OIrO? Scale factors for OIrO were 0.96 and 0.94 using the D95* basis set. Scale factors for RhO and ORhO from a similar investigation were 0.95 and 0.94, respectively. For Ir−O and Rh−O stretching modes, the BPW91/D95*/LanLECP calculated frequencies are approximately 5% too high. Replacing the D95* basis set on oxygen with the 6-311+G(d) basis set improves the description of charge distribution and brings the scale factors closer to unity. These calculations provide a good starting point for subsequent ab initio calculations.

References and Notes

(1) Andrews, L.; Chertihin, G. V.; Ricca, A.; Bauschlicher, C. W., Jr. *J. Am. Chem. Soc.* **1996**, *118*, 467.
(2) Crabtree, R. H. *Chem. Rev.* **1985**, *85*, 245.
(3) Holm, R. H. *Chem. Rev.* **1987**, *87*, 1401.
(4) Hassanzadeh, P.; Andrews, L. *J. Phys. Chem.* **1992**, *96*, 9177.
(5) Chertihin, G. V.; Andrews, L. *J. Phys. Chem.* **1995**, *99*, 6356.
(6) Chertihin, G. V.; Citra, A.; Andrews, L.; Bauschlicher, C. W., Jr. *J. Phys. Chem. A* **1997**, *101*, 8793.
(7) Frisch, M. J.; Trucks, G. W.; Schlegel, H. B.; Gill, P. M. W.; Johnson, B. G.; Robb, M. A.; Cheeseman, J. R.; Keith, T.; Petersson, G. A.; Montgomery, J. A.; Raghavachari, K.; Al-Laham, M. A.; Zakrzewski, V. G.; Ortiz, J. V.; Foresman, J. B.; Cioslowski, J.; Stefanov, B. B.; Nanayakkara, A.; Challacombe, M.; Peng, C. Y.; Ayala, P. Y.; Chen, W.; Wong, M. W.; Andres, J. L.; Replogle, E. S.; Gomperts, R.; Martin, R. L.; Fox, D. J.; Binkley, J. S.; Defrees, D. J.; Baker, J.; Stewart, J. P.; Head-Gordon, M.; Gonzalez, C.; Pople, J. A. *Gaussian 94*, revision B.1; Gaussian, Inc.: Pittsburgh, PA, 1995.
(8) Becke, A. D. *Phys. Rev. A* **1988**, *38*, 3098.
(9) Perdew, J. P.; Wang, Y. *Phys. Rev. B* **1992**, *45*, 13244.
(10) Hay, P. J.; Wadt, W. R. *J. Chem. Phys.* **1985**, *82*, 299.
(11) Reed, A. E.; Curtiss, L. A.; Weinhold, F. *Chem. Rev.* **1988**, *88*, 899.
(12) Jansson, K.; Scullman, R. *J. Mol. Spectrosc.* **1972**, *43*, 208.
(13) Jansson, K.; Scullman, R. *Ber. Bunsen-Ges. Phys. Chem.* **1978**, *82*, 92.
(14) Campbell, M. L. *J. Phys. Chem. A* **1997**, *101*, 9377.
(15) Wilson, E. B., Jr.; Decius, J. C.; Cross, P. C. *Molecular Vibrations; The Theory of Infrared and Raman Vibrational Spectra*; McGraw-Hill: New York, 1955.
(16) Allavena, M.; Rysnik, R.; White, D.; Calder, V.; Mann, D. E. *J. Chem. Phys.* **1969**, *50*, 3399.
(17) Van Zee, R. J.; Hamrick, Y. M.; Li, S.; Weltner, W., Jr. *J. Phys. Chem.* **1992**, *96*, 7247.
(18) Hayes, E. F. *J. Phys. Chem.* **1966**, *70*, 3740.
(19) Citra, A.; Andrews, L. *J. Phys. Chem. A*, in press.
(20) Bytheway, I.; Wong, M. W. *Chem. Phys. Lett.* **1998**, *282*, 219.
(21) Neuhaus, A.; Veldkamp, A.; Frenking, G. *Inorg. Chem.* **1994**, *33*, 5278.
(22) Chertihin, G. V.; Bare, W. D.; Andrews, L. *J. Phys. Chem. A* **1997**, *101*, 5090.
(23) Zhou, M. F.; Andrews, L. *J. Phys. Chem. A* **1998**, *102*, 8251.
(24) Hope, E. G.; Levason, W.; Ogden, J. S.; Tajik, M. *J. Chem. Soc., Dalton Trans.* **1986**, *8*, 1587.
(25) Kettle, S. F. A.; Paul, I. *Adv. Organomet. Chem.* **1972**, *10*, 199.
(26) Geoffroy, G. L.; Hammond, G. S.; Gray, H. G. *J. Am. Chem. Soc.* **1975**, *97*, 3933.
(27) Cotton, F. A.; Wilkinson, G. *Advanced Inorganic Chemistry*, 5th ed; Wiley: New York, 1988.
(28) Frenking, G.; Pidun, U. *J. Chem. Soc., Dalton Trans.* **1997**, *10*, 1653.
(29) McGhee, W. D.; Foo, T.; Hollander, F. J.; Bergman, R. G. *J. Am. Chem. Soc.* **1988**, *110*, 8543.
(30) Vaartstra, B. A.; Xiao, J.; Cowie, M. *J. Am. Chem. Soc.* **1990**, *112*, 9425.
(31) Choy, V. J.; O'Conner, C. J. *Coord. Chem. Rev.* **1972/1973**, *9*, 145.
(32) Choy, J. H.; Kim, D. K.; Hwang, S. H.; Demazeau, G.; Jung, D. Y. *J. Am. Chem. Soc.* **1995**, *117*, 8557.
(33) Bellon, P. L.; Benedicenti, C.; Caglio, G.; Manassero, W. *J. Chem. Soc., Chem. Commun.* **1973**, 946.
(34) Mason, R.; Sotofte, I.; Robinson, S. D.; Uttley, M. F. *J. Organomet. Chem.* **1972**, *46*, C61.
(35) Huber, H. H.; Klotzbucher, W. E.; Ozin, G. A.; Vander Voet, A. *Can. J. Chem.* **1973**, *51*, 2722.